Theoretical and Applied Climatology
https://doi.org/10.1007/s00704-022-04195-1

ORIGINAL PAPER

Global trends in the occurrence and characteristics of blocking anticyclones using Şen innovative trend analysis

Bahtiyar Efe[1] · **Anthony R. Lupo**[2]

Received: 20 May 2021 / Accepted: 29 August 2022

Abstract
Atmospheric blocking plays an important role in modulating mid-latitude weather, particularly for the Northern Hemisphere (NH). Trend analysis of atmospheric blocking for both hemispheres using Şen's innovative trend analysis (ITA) is performed here. The blocking data archived at the University of Missouri which covers the period of 1968–2019 for NH and 1970–2019 for the Southern Hemisphere (SH) is used in this study. Block occurrence (BO), duration (BD), and blocking intensity (BI) are analyzed by classifying the NH (SH) into three groups according to the preferred block formation locations: Atlantic, Pacific, and Continental (Atlantic, Pacific, and Indian). In the NH, BI showed mixed results. There was a decreasing trend for the entire hemisphere and Atlantic Region while different trends were observed elsewhere. For BO and BD, the entire hemisphere and all regions showed increasing trends, which were statistically significant. In SH, BI shows a decreasing trend for weaker blocking events while medium and high clusters for the entire hemisphere. The BD exhibited an increasing trend for the entire SH. The BO also showed an increasing trend except one point in less active years. Blocking characteristics show different trends for different preferred blocking locations. Increasing trends of SH BO for the overall sample and Pacific Region are statistically significant at 95% level. Increasing trends for SH BD overall and in the Atlantic and Pacific regions are statistically significant at 90%, 95%, and 95% levels, respectively.

1 Introduction

Different aspects of blocking anticyclone character and dynamics have been studied due to their important contributions to atmospheric phenomena like droughts, heavy precipitation (Khodayar et al. 2018; Rabinowitz et al. 2018), heat waves (Sitnov et al. 2014; Lhotka et al. 2018), and cold spells (O'Reilly et al. 2016; Aalijahan et al. 2018; Brunner et al. 2018). These extremes have an adverse effect on daily life. Some studies focused on blocking indicators (Lejenas and Okland 1983; Tibaldi and Molteni 1990 (hereafter TM90); Lupo and Smith 1995; Barriopedro et al. 2006); the relationship between blocking and meteorological variables (Rabinowitz et al. 2018; Efe et al. 2019, 2020a,b; Canyilmaz 2020), and predictability (TM90; Matsueda 2011).

Interdecadal variability and long-term trends of atmospheric blocking for both hemispheres are also studied by researchers (Wiedenmann et al. 2002; Barriopedro et al. 2006; Mokhov et al. 2012; Barnes et al. 2014; Lupo et al. 2019). Studies covering the period of the late twentieth century for Northern Hemisphere (NH) blocking events showed that long-term trends depend on the season and region (Wiedenmann et al. 2002). Barriopedro et al. (2006) demonstrated that these mixed results are due to interdecadal variations related to teleconnection patterns such as those associated with North Atlantic Oscillation (NAO) and Western Pacific (WP) Index. However, Lupo et al. (2019) showed that block occurrence (BO) has decreased to a minimum in the late twentieth century by examining the blocking data time series up to 2018. They found evidence of an increase in BO since the beginning of the twenty-first century.

For the Southern Hemisphere (SH), Wiedenmann et al. (2002) showed that BO and duration (BD) decreased strongly during the last part of the twentieth century that was consistent with Renwick and Revell (1999). However, Oliveria et al. (2014) found no statistically significant trend within the whole SH that covers a longer period. Lupo et al. (2019) demonstrated that BO and BD had increased significantly for the SH at the start of the twenty-first century.

✉ Bahtiyar Efe
bahtiyar.efe@samsun.edu.tr

[1] Department of Meteorological Engineering, University of Samsun, 19 Mayis, Samsun, Turkey

[2] Atmospheric Science Program, School of Natural Resources, University of Missouri, Columbia, USA

Published online: 06 September 2022

The Şen innovative trend analysis method (hereafter ITA) (Şen 2012) is a technique by which the trend is detected visually. It is a widely used method in environmental sciences. Şen and Aksu (2021) used ITA to detect a trend in maximum precipitation in İstanbul, the largest city of Turkey. Cui et al. (2017) investigated the trend analysis of annual and seasonal air temperature and rainfall in the Yangtze River Basin in China by using ITA. Tosunoglu and Kisi (2017) applied ITA in order to detect trends in hydrologic drought variables in Çoruh River Basin, Turkey. Phuong et al. (2022) detected trends in Standard Precipitation Index in the Central Highlands of Vietnam by using ITA. ITA is used to detect trends in water quality as well (Moravej et al. 2018). However, the ITA method has not been used in atmospheric blocking studies.

Our study is unique in that it uses the ITA to detect trends for the variables BO, BD, and blocking intensity (BI). Both the Northern and Southern hemispheres are considered for trend detection. While inferred trends have been published in studies of BO and for other blocking characteristics by this research group previously, the goal of this work is to apply ITA for blocking character in order to determine whether ITA supports these previously published results. Additionally, the ITA analysis can provide more information about these trends. For example, ITA will demonstrate whether trends in the block intensity are most notable among weak, typical or moderate, and strong blocking events. Lastly, this work will use the Mann–Kendall tau test for trends, which is more proper than the techniques used to infer trends in Lupo et al. (2019).

2 Data and methodology

The blocking data used in this study are archived in the University of Missouri Blocking Archive (2020), and the variables used here include the blocking intensity, duration, and occurrence. The blocking data used in this study covers the period from 1968 to 2019 for NH and 1970–2019 for SH. The blocking year starts in July for NH and January for SH as in Lupo et al. (2019) and references therein. The trend for blocking parameters was investigated for the whole hemisphere and then for different preferred blocking regions within both hemispheres. In NH, there are three preferred blocking regions: Atlantic (80° W–40° E), Pacific (140° E–100°W), and Continental (100°–80° W and 40°–140°E). The SH has also three preferred regions: Atlantic (60° W–30° E), Pacific (130° E–60° W), and Indian (30°–130° E). In the NH, blocking has been observed at least one time each year in all regions. In the SH, the Pacific Region has blocking events for all years while the other regions do not have blocking events observed for some years. Thus, the deficient years are included into the lower cluster which will be described later. Then, the lower cluster is ignored due to there being few members for the Atlantic and Indian Ocean region samples. This dataset has been used in numerous studies (e.g., Lupo et al. 2019; Efe et al. 2020a, b; and references therein).

The Şen innovative trend analysis method (Şen 2012) which is a non-parametric trend test was used to describe trends in blocking parameters. This method is composed of several steps. First, the data is separated into two equal parts (e.g., for NH, 1968–1993 is the first or earlier period and 1994–2019 is the second or later). Then, the data is sorted in an ascending order for both halves (e.g., BI is sorted from the lowest to the highest value in the first period and second period). The next step is plotting the scatter of these ordered data in a Cartesian coordinate system and the 1:1 (trend free) line is added. The ordered data in the first half is located on the abscissa and the second half is located on the ordinate. If the data are trend free, the points fall on the 1:1 line. If there is an increasing trend, the points fall in the upper triangle while they all fall in the lower triangle for the decreasing trend. For the monotonic increasing (decreasing) trend, the points fall on another line in the upper (lower) triangle parallel to the 1:1 line. If the trends are non-monotonic, they fall on the line not parallel to the 1:1 line or they have mixed behavior for the trend. The methodology is based on the visualization of the data. The scatter points are clustered as low, medium, and high. For BI, weaker blockings, moderate blockings, and stronger blockings are used to define the low, medium, and high clusters, respectively. For BD, less persistent blockings, typical blockings, and more persistent blockings are used to define low, medium, and high clusters, respectively. More persistent blocking means an event with a longer duration in days. For BO, less active years, typical years, and more active years are used to define low, medium, and high clusters, respectively. The BI clusters are defined according to Lupo and Smith (1995). The BO and BD clusters are subjectively determined. The reason for clustering is to examine the trend in more detail than for previously published results. The trend magnitude of any point is described as the distance between the point and the 1:1 trend line. All figures are illustrated via ggplot2 R-package (Wickham 2016). All necessary data transformations and basic calculations are done via base R and dplyr packages of R (R Core Team 2018; Wickham et al. 2018).

The non-parametric Mann–Kendall tau test which is a widely used trend test in atmospheric sciences is also applied to detect the statistical significance of trends (Kendall 1975). Positive values of tau indicate an increasing trend while negative values indicate a decreasing trend. The p-value is used to detect statistical significance in the Mann–Kendall test. If the p-value is smaller than 0.05, the trend is statistically significant at the 95% significance level. The characteristics of blocking data for both hemispheres are checked for serial independence using the autocorrelation function. BI, BD, and BO do not have serial correlations for both hemispheres.

3 Results

3.1 Northern Hemisphere

3.1.1 Entire hemisphere

For the NH, the long-term average of annual blocking numbers is 24.5 for the first period and 37.2 for the second period. The trend for the annual average of BI in the NH is shown in Fig. 1. All three clusters of BI values are scattered within the lower triangle, and this means the BI has a decreasing trend for all clusters. In the weaker blocking events, there is a non-monotonic decreasing trend. The trend magnitude is highest for the lower portion of the weaker blocking events, but it is slight in the upper parts. The medium blocking events have a monotonic decreasing trend with a magnitude greater than stronger blockings and lower than weaker blockings. The stronger blocking events have a monotonic decreasing trend with the least trend magnitude of all three clusters.

The scatter diagram of the BD annual average between the earlier and later part of the study period is shown in

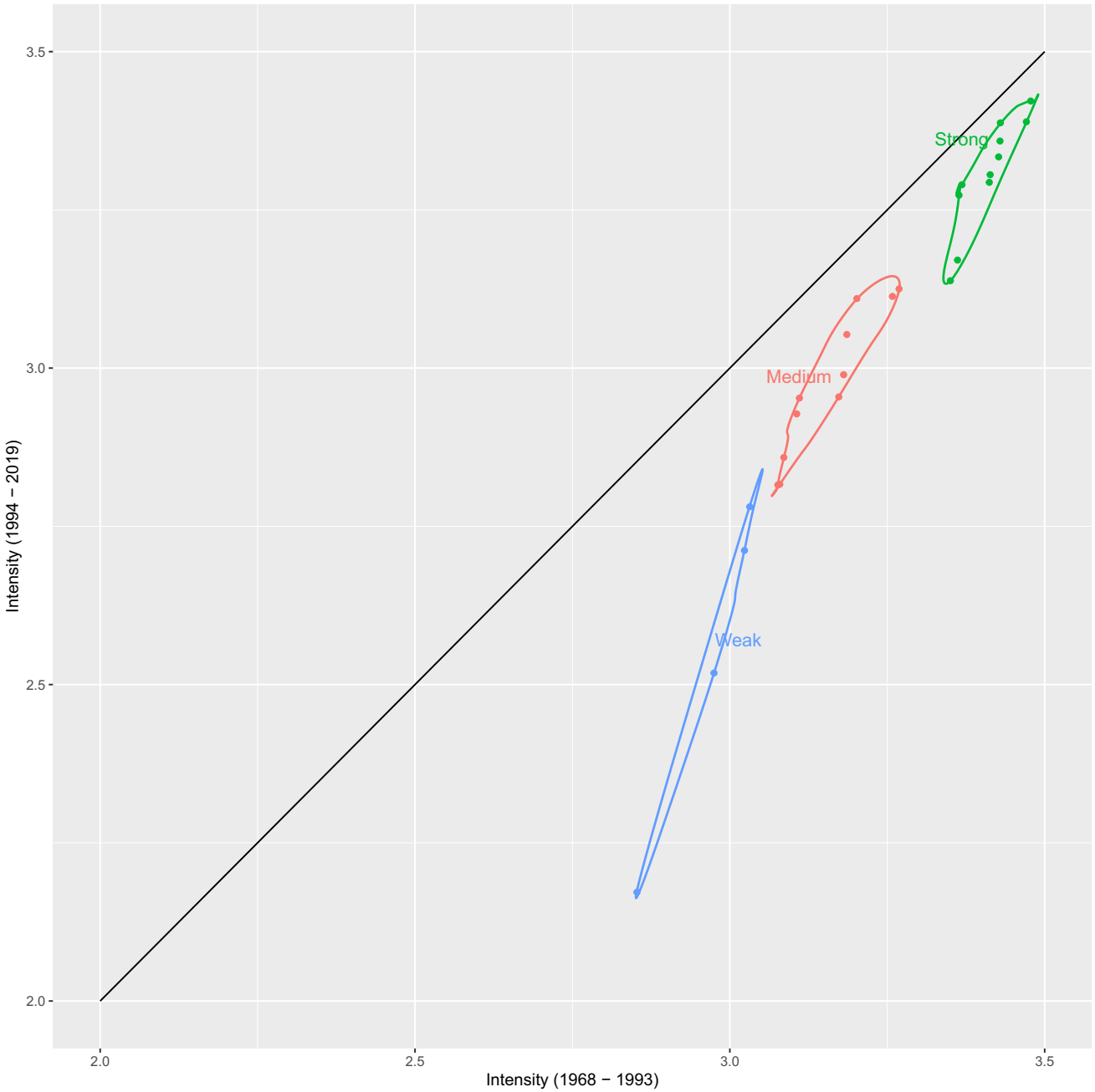

Fig. 1 BI trend analysis for the NH using the Şen ITA

Fig. 2, where the BD has an increasing trend for the whole hemisphere for all clusters. The BD has a non-monotonic trend for all data. The less persistent blockings have a monotonic increasing trend with less departure from the 1:1 line. The medium cluster has a greater departure from the 1:1 line than less persistent events, and it has a non-monotonic increasing trend. The departure for the higher portion of the medium cluster is greater than for the lower parts. The most persistent blockings have the largest departure values than the medium cluster with a monotonic increasing trend.

As seen in Fig. 3, the annual number of blocking events is increasing for all clusters. All the points fall into the upper triangle with no exception. The trend is non-monotonic for blocking numbers. The less active years have a relatively small magnitude of trend with an increasing magnitude which means it has a non-monotonic increasing trend. The medium years have a non-monotonic increasing trend with increasing magnitude. The more active years have a monotonic increasing trend. Overall, the magnitude of trends increases by the magnitude of the cluster.

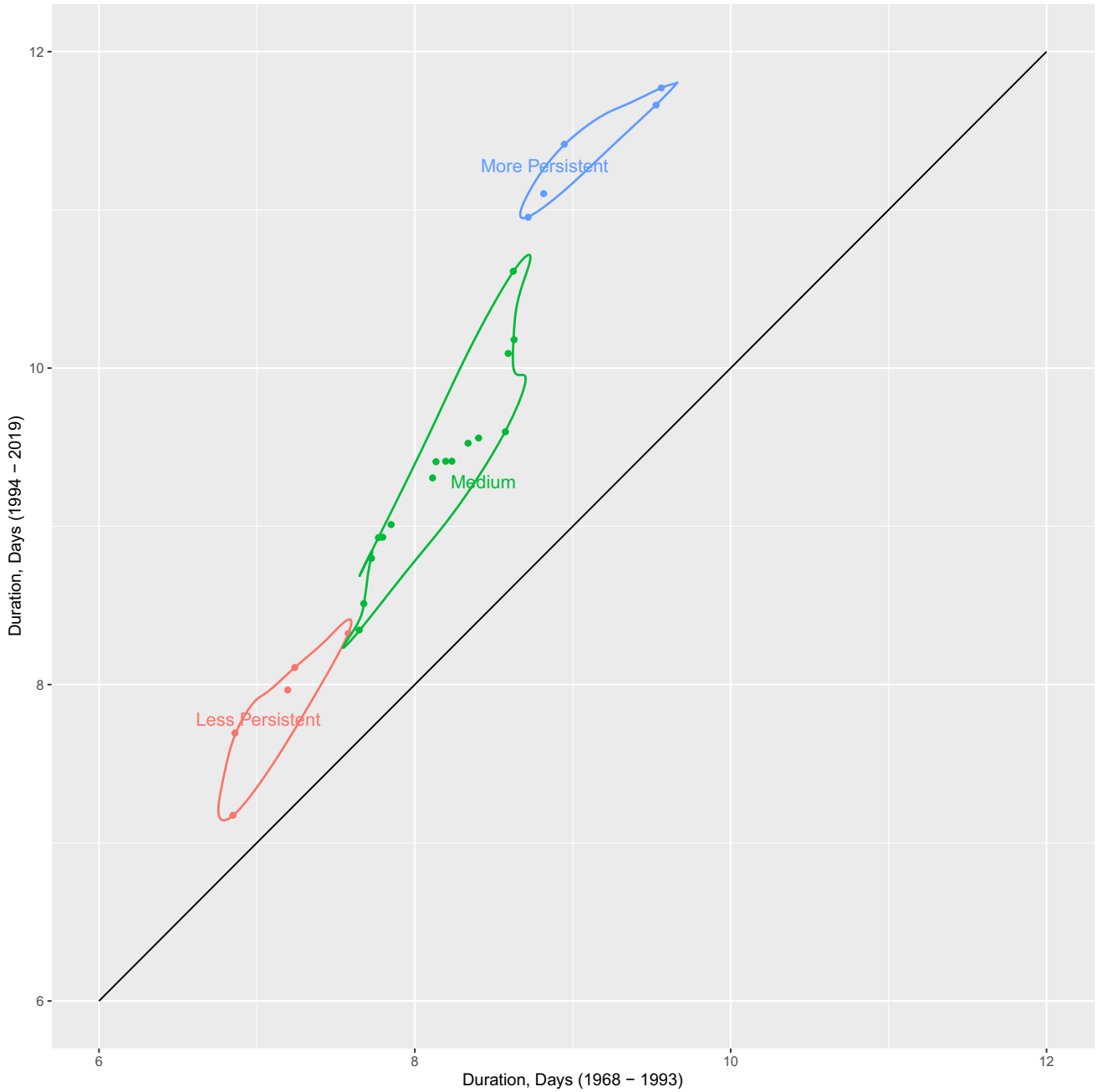

Fig. 2 As in Fig. 1, except for block duration

3.1.2 Preferred blocking locations

For the Atlantic Region, the long-term annual average for blocking occurrences is 12.8 in the earlier period and 15.8 in the later period. The corresponding values for the Pacific and Continental regions are 6.3 and 5.4, respectively, in the earlier period and 11.8 and 9.6, respectively, for the later period. The scatter plot of the two periods for BI annual average stratified by preferred blocking regions is seen in Fig. 4. The Atlantic Region has decreasing trends for all three clusters. However, the magnitude is higher in the lower portion of the weaker blocking events. The samples for the other clusters are located near the 1:1 line. In the Pacific Region, the trend behavior is different for all clusters. The weaker blockings have an increasing trend while typical events are closer to the trend-free line. The lower part of stronger blockings has an increasing trend with low magnitudes and the upper part has a decreasing trend. The Continental Region has also mixed trend types. The stronger and typical blockings have decreasing trends while weaker

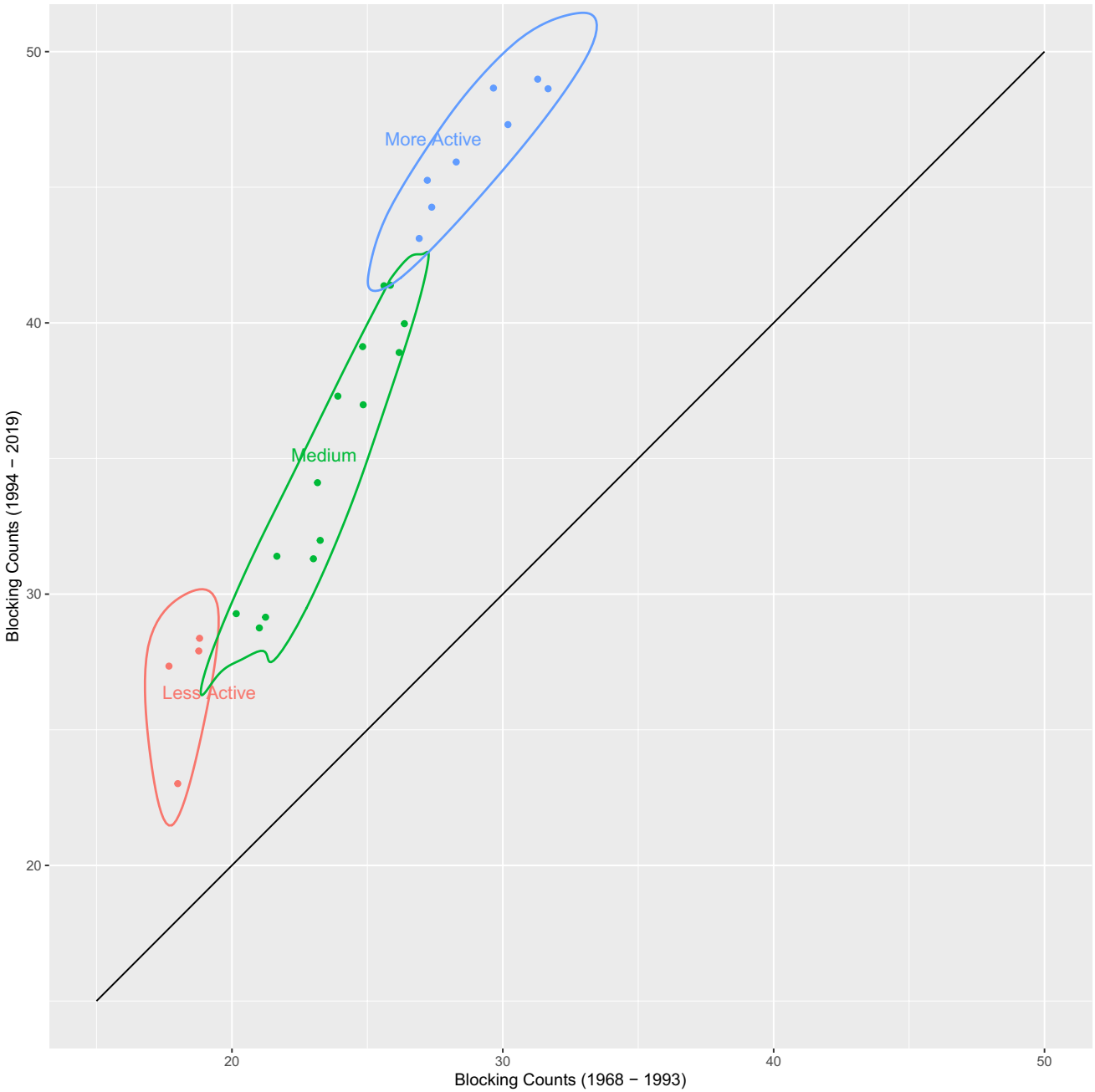

Fig. 3 As in Fig. 1 except for block occurrences

blockings have decreasing trends for higher values and increasing trends for lower values.

The trend analysis for the annual BD average within different blocking regions can be seen in Fig. 5. For the Atlantic Region, the mean duration has a non-monotonic increasing trend; the higher the cluster, the higher the trend magnitude. Although the lowest value of the less persistent events has a decreasing trend, the Pacific Region has almost a monotonic increasing trend behavior. All three clusters have an increasing trend with similar magnitude except at the higher part of the more persistent events. The more persistent blockings have a slightly higher magnitude of trend. The less persistent blockings and medium blockings of mean BD have an increasing trend for the Continental Region with smaller trend magnitudes. On the other hand, more persistent events are trend free for lower values while it has an increasing trend for higher values.

The annual number of blocking events for the preferred regions in the NH is seen in Fig. 6. All three regions have an increasing trend for all three clusters with no exception. The Atlantic Region has an increasing trend for all three clusters. However, the clusters have different trend magnitudes. Less active years have an increasing trend around the 1:1 line. Typical years have a non-monotonic increasing trend with increasing magnitude. More active years have a monotonic increasing trend. The Pacific Region has a monotonic trend for typical and more active years. Less active years have a non-monotonic increasing trend with an increasing trend magnitude. The Continental Region has an almost monotonic increasing trend. The trend magnitude slightly increases up to typical years than decreases back in the more active years.

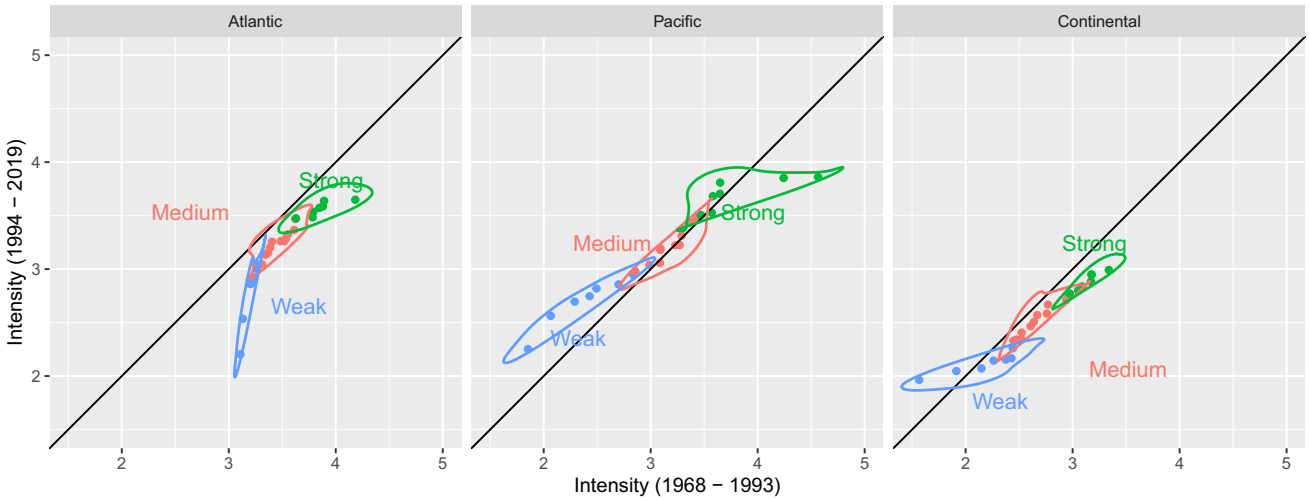

Fig. 4 As in Fig. 1, but stratified by preferred blocking locations

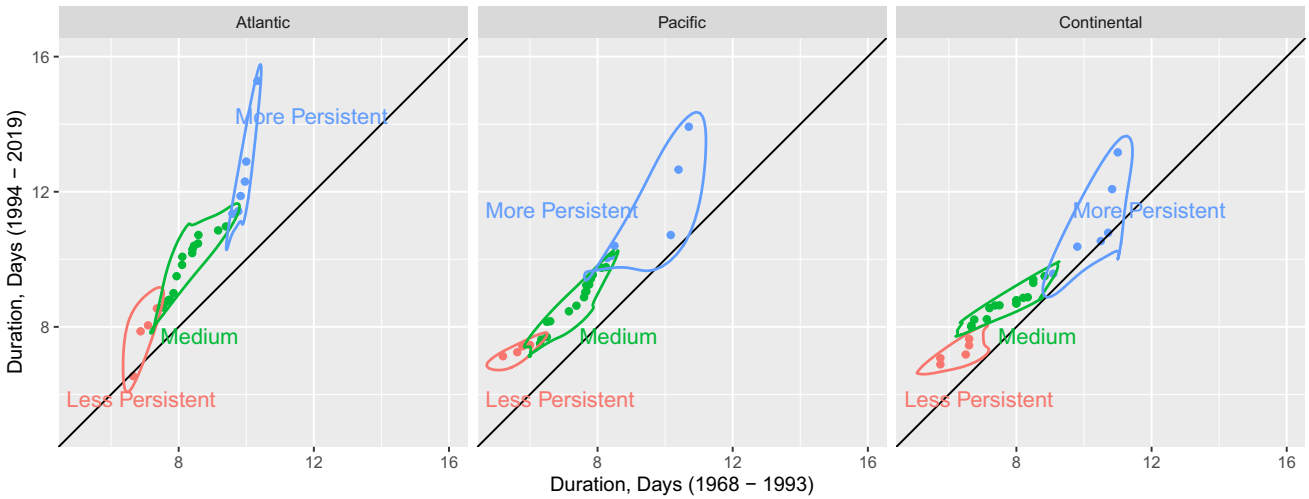

Fig. 5 As in Fig. 2, but stratified by preferred blocking locations

3.1.3 Mann–Kendall trend analysis

Mann–Kendall tau values are shown in Table 1. The BI for the Continental Region has a statistically significant decreasing trend at 90% ($p=0.10$) confidence level. BO and BD had a statistically significant increasing trend at the 99% ($p=0.01$) level for the whole hemisphere and preferred blocking locations. The test used here to identify trends is more appropriate than those used in Lupo et al. (2019). They tested the means of the early twenty-first century blocking characteristics versus those of the late twentieth century. Their test suggested generally the BI decreases were more significant than those found here, while the BD increases were less significant. For BO, the techniques used here and in Lupo et al. (2019) give the same conclusion.

Bold values indicate $0.05 < p < 0.1$; bold* indicates $0.01 < p < 0.05$; bold** indicates $p < 0.01$.

3.2 Southern Hemisphere

3.2.1 Whole hemisphere

For the SH, the long-term annual average blocking numbers are 10.2 for the earlier period and 15.0 for the later period. The scatter plot of the two halves for the BI annual average is seen in Fig. 7. The BI has a different trend behavior for different clusters. The weaker events have mixed trend types around the trend-free line. The typical events have a decreasing trend at the lowest values and a non-monotonic increasing trend for the rest of the values with increasing trend magnitude. The strongest blockings have a monotonic increasing trend.

The annual average of the mean BD has an increasing trend with interesting behavior (Fig. 8). All three clusters have an increasing trend. The less persistent events have the same magnitude of trend for all their elements, meaning it has a monotonic increasing trend. The medium cluster has a greater trend magnitude for the lower part and the higher part has a lower trend magnitude. For the more persistent blockings, the magnitude of the increasing trend increases by the higher values. The highest points display the highest trend magnitudes.

The annual number of the blocking events in SH is plotted in Fig. 9. The less active years have an increasing trend with a lower trend magnitude except one point. That point fell into the lower triangle. The medium years have an increasing trend with increasing magnitude. The more active years have a monotonic increasing trend.

3.2.2 Preferred blocking locations

In the Atlantic Region, the long-term block occurrence average is 1.0 for the earlier period versus 1.4 for the later

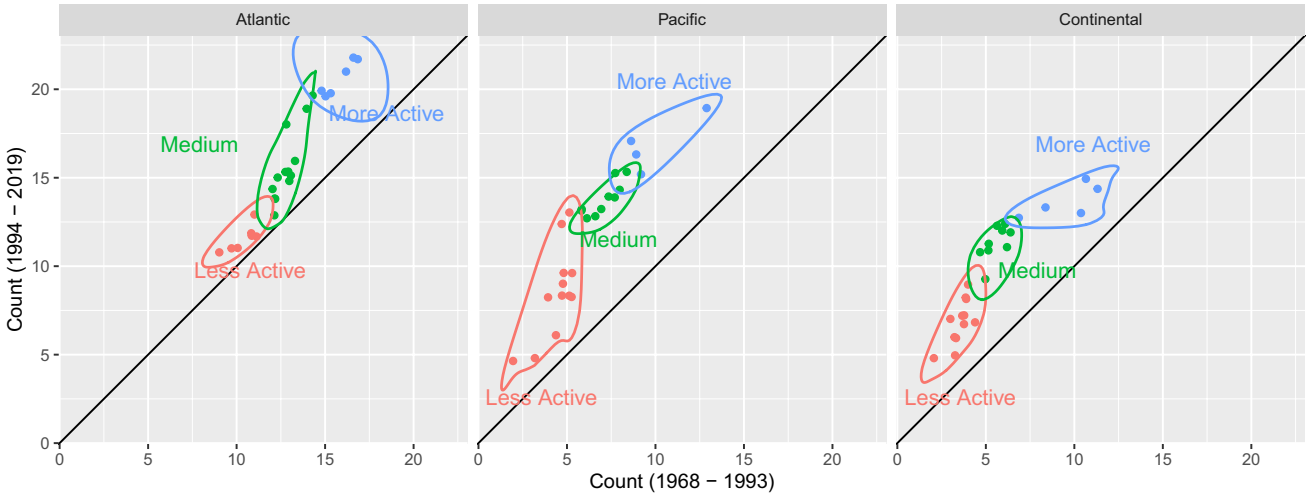

Fig. 6 As in Fig. 3, but stratified by preferred blocking locations

Table 1 Mann–Kendall tau values for whole NH and preferred blocking locations

	Northern Hem	Atlantic Region	Pacific Region	Continental Region
Blocking intensity	−0.15	−0.14	0.005	**−0.18**
Blocking number	**0.52****	**0.33****	**0.45****	**0.49****
Blocking duration	**0.37****	**0.37****	**0.34****	**0.25****

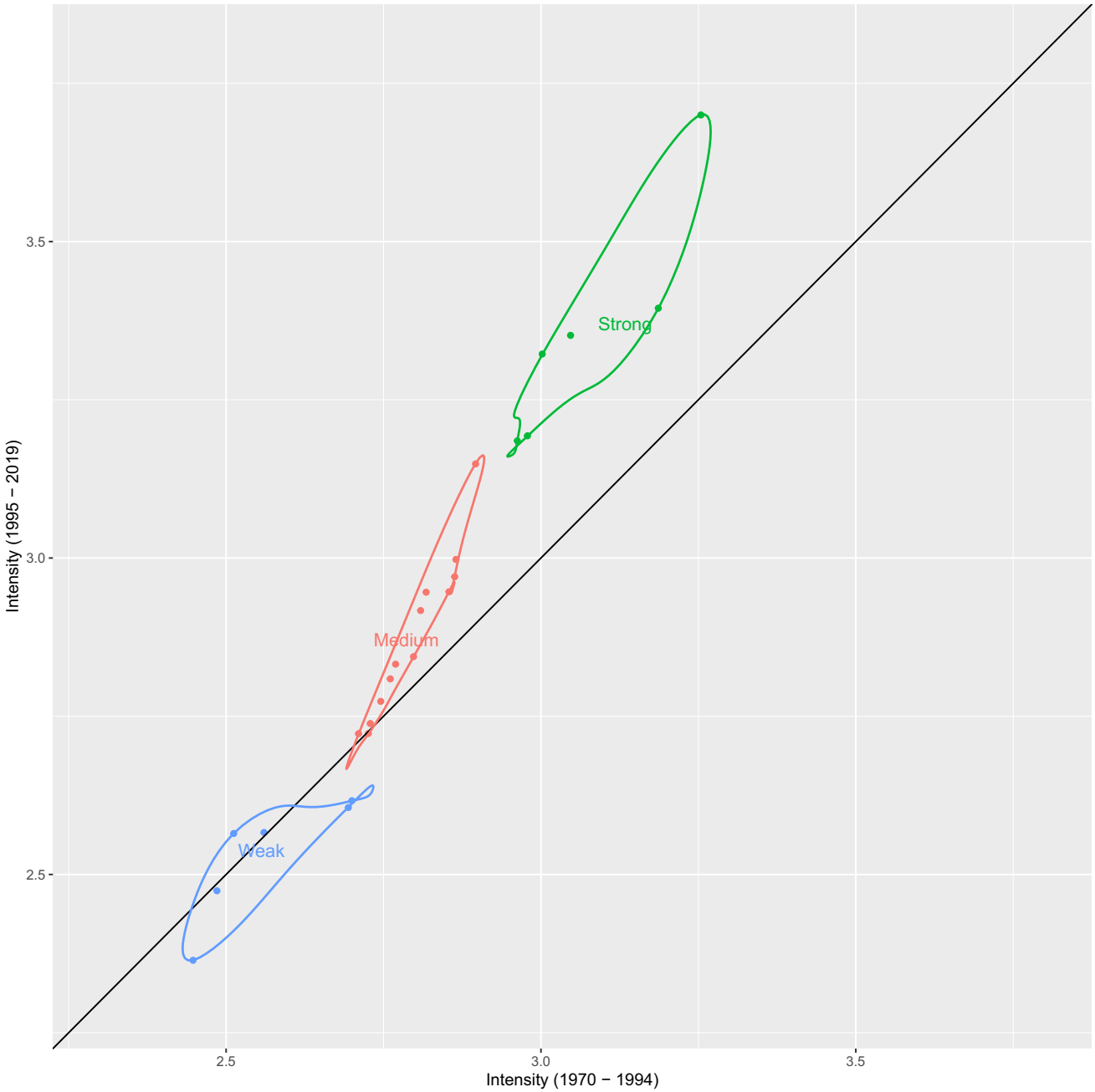

Fig. 7 As in Fig. 1, except for the SH

period. For the Pacific Region, the long-term block occurrence average is 8.2 for the earlier period versus 11.3 for the later period. For the Indian Ocean Region, the long-term block occurrence average is 1.0 for the earlier period versus 2.2 for the later period.

The trend in the annual BI average for preferred blocking regions can be seen in Fig. 10. For the Atlantic Region, the mean BI has an increasing trend for the lower part of typical events while it has a decreasing trend for higher values. The stronger events have a mixed trend of decreasing, increasing, and no trend. It has no trend for the lower part, decreasing for middle values, and increasing for higher. In the Pacific Region, all three clusters have an increasing trend with lower trend magnitudes. The higher part of the weaker events and the lower part of typical events show points on the trend-free line. The higher part of stronger blockings has the greatest increasing trend. For the Indian Region, the lower values of typical events have an increasing trend and the higher values have a decreasing trend. The stronger blocking events have a monotonic increasing trend with a small trend magnitude.

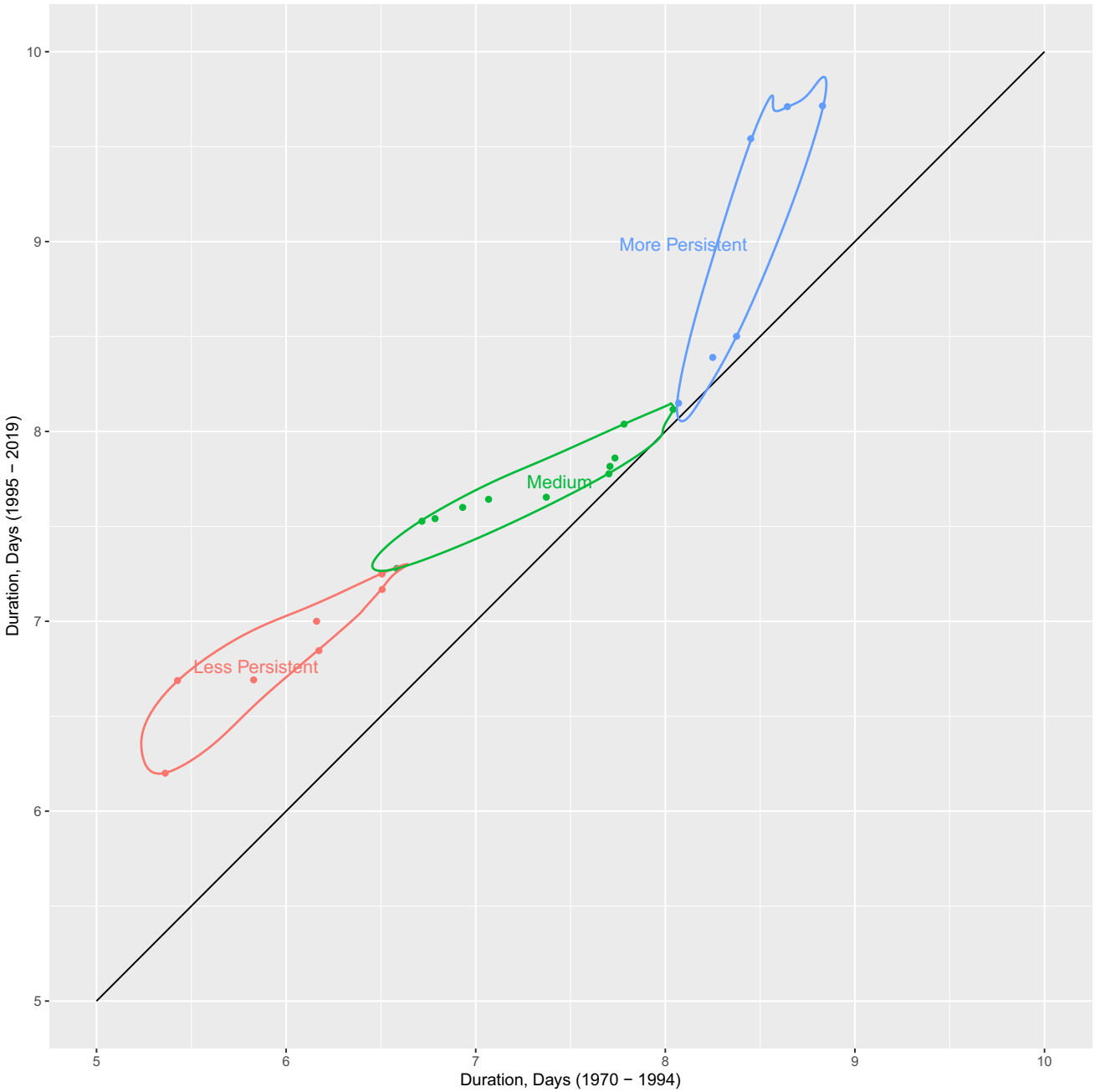

Fig. 8 As in Fig. 2, except for the SH

The scatter plot for the two halves of the annual BD average for three locations within the SH is seen in Fig. 11. For the Atlantic Region, BD has a monotonic increasing trend with a small magnitude for the medium cluster with some points along the trend-free line. The more persistent blockings have an increasing trend generally. In the Pacific Region, the less persistent events have a monotonic increasing trend. The medium cluster has an increasing trend with a decreasing magnitude of trend, while the more persistent events have contrasting behavior within the medium cluster. For the Indian Region, the medium cluster has an increasing trend with decreasing magnitude. The more persistent events have a decreasing trend with lower values and an increasing trend for the highest value of the high cluster.

The annual occurrence of blocking events for the preferred regions within the SH is seen in Fig. 12. Each of the three regions has different behaviors. The Atlantic Region has no trend for small values of typical years and then an

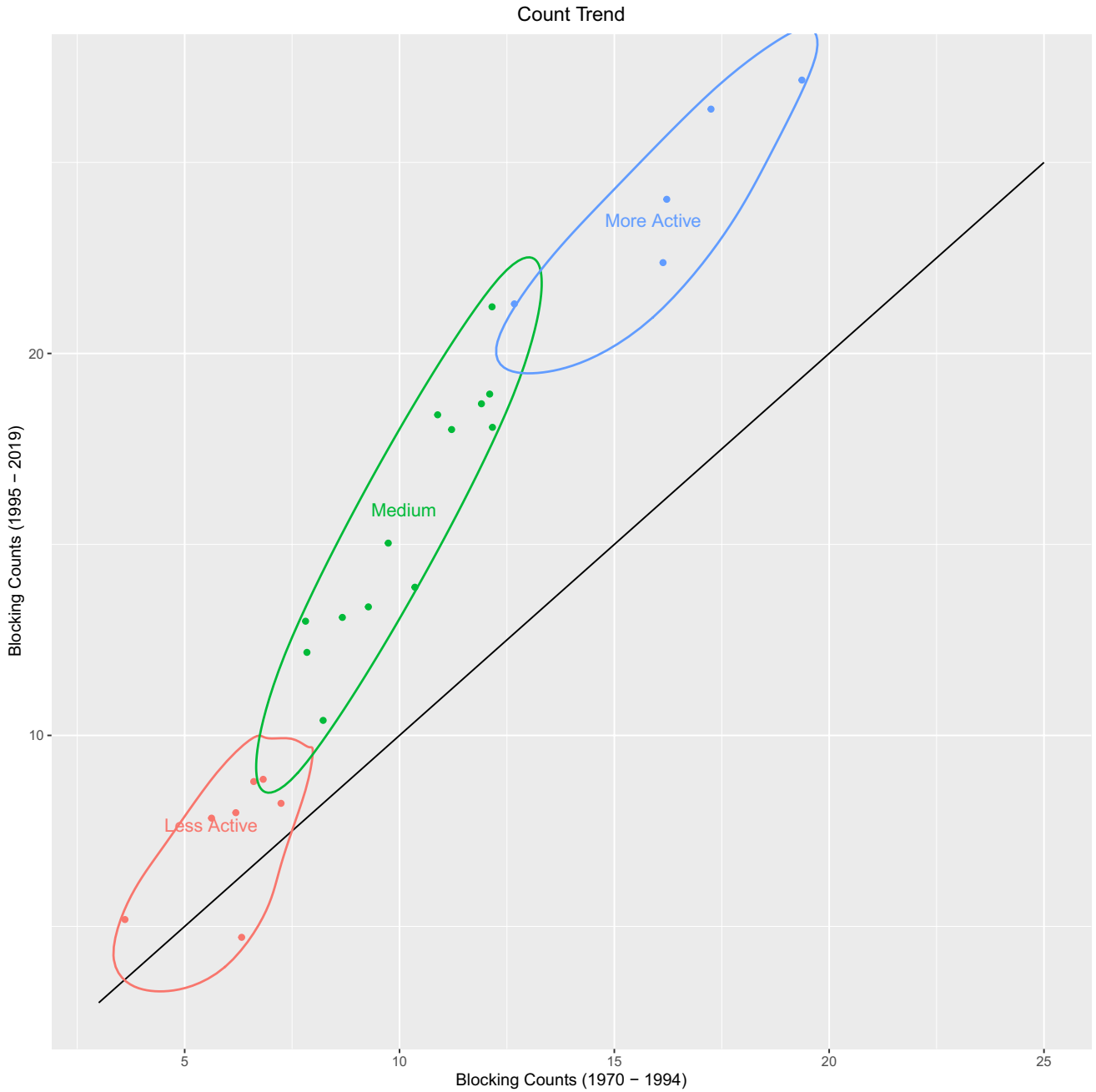

Fig. 9 As in Fig. 3, except for the SH

increasing trend for higher values with low magnitudes. The active years have a decreasing trend for small values and an increasing trend for high values with low magnitudes of trend. The Pacific Region has an increasing trend for almost all three clusters. Less active years have little trend and the lowest portion of the cluster and then an increasing trend of low magnitude. Medium years have a monotonic increasing trend with the magnitude greater than less active years. More active years have an increasing trend with increasing trend magnitude. The Indian Region has a decreasing trend for small values of medium years, then an increasing trend for higher values within the cluster. More persistent years have an increasing trend for lower values and the magnitude of trend decreases and then touches the no-trend line at the highest point.

3.2.3 Mann–Kendall trend analysis test

The Mann–Kendall tau values are shown in Table 2. BI does not have a statistically significant trend not only for the whole SH

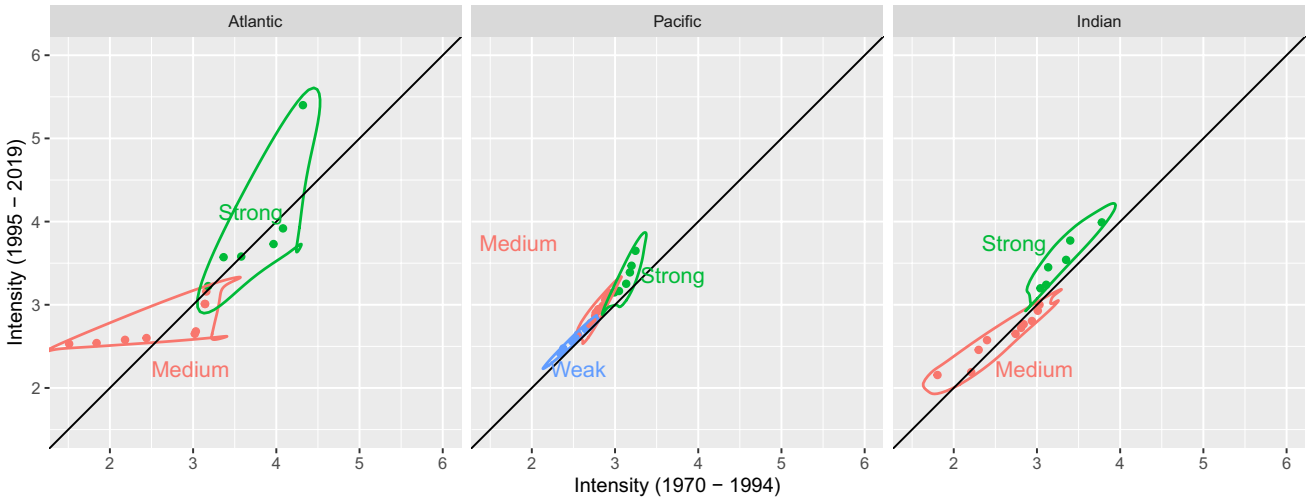

Fig. 10 As in Fig. 7, but stratified by preferred blocking locations

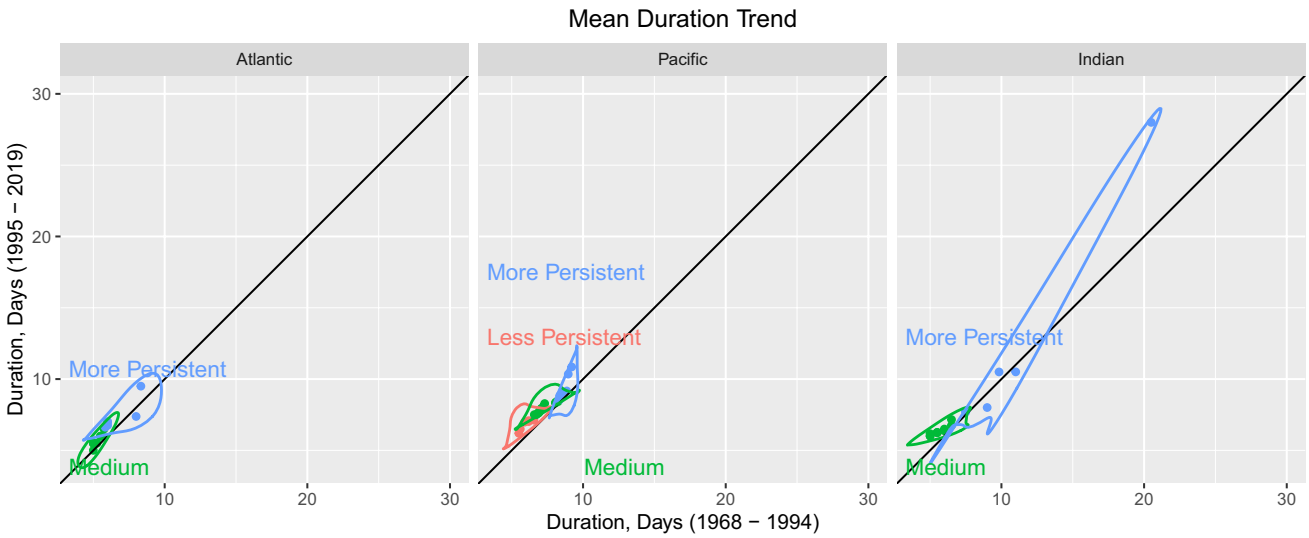

Fig. 11 As in Fig. 8, but stratified by preferred blocking locations

hemisphere but also preferred blocking locations. The Lupo et al. (2019) results did infer significant decreases for BI in the Atlantic and Indian Ocean regions. BO showed a statistically significant increasing trend at 99% confidence level for the whole hemisphere and Pacific Region. This is similar to Lupo et al. (2019); however, they also showed significant increases in the Atlantic and Indian Regions. The latter result is not supported here. BD has a statistically significant increasing trend at 90% level for the whole hemisphere and at 95% ($p=0.05$) confidence level for the Atlantic and Pacific regions. For BD, the only difference from Lupo et al. (2019) was the significant increase in the Atlantic Region.

Bold values indicate $0.05 < p < 0.1$; bold* indicates $0.01 < p < 0.05$; bold** indicates $p < 0.01$.

4 Discussion

The Şen ITA analysis performed here reexamines the trends found in an earlier climatological study (Lupo et a. 2019) which used traditional analysis of variance (ANOVA) techniques. As shown in Sect. 3, the NH and SH decreases in BI were less significant than those found in Lupo et al. (2019), while the increases in NH durations here were more significant. In the SH, the increased occurrence within the Atlantic and Indian Ocean regions was not significant here, where blocking occurs much less frequently. This may be a function of the small sample size for these regions. However, where the two statistical methods show similar significance increases our confidence

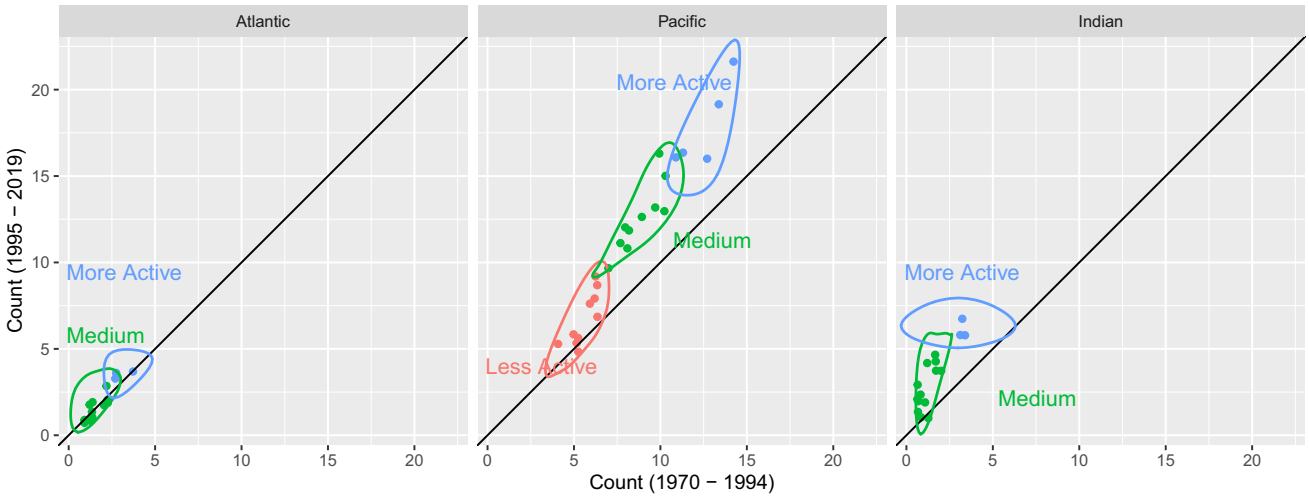

Fig. 12 As in Fig. 9, but stratified by preferred blocking locations

Table 2 Mann–Kendall tau values for the whole Southern Hemisphere and preferred blocking locations

	Southern Hem	Atlantic Region	Pacific Region	Indian Region
Blocking intensity	0.04	0.07	0.11	0.001
Blocking number	**0.34****	0.17	**0.34****	0.15
Blocking duration	**0.17**	**0.22***	**0.20***	0.07

in those findings. Thus, the differences in the significance of blocking character changes found here versus those found in Lupo et al. (2019) show that the strength of our confidence can be a function of the statistical technique chosen even for the same data set. This type of result is not unique. Additionally, comparing blocking data sets using different definitions (e.g., Pinhero et al. 2019) will produce different results as well. However, the Şen ITA analysis provides also for a simpler method in examining the overall trends of blocking character in greater detail than shown in Lupo et al. (2019).

Lupo and Smith (1995) and references therein showed a dynamic connection between upstream extratropical cyclones in supporting the formation and persistence of blocking. They demonstrated that there was a significant correlation between the deepening rate of these NH extratropical cyclones and block intensity, as well as a correlation between NH duration and block intensity. The duration and BI correlation was supported by Lupo et al. (2019). In the SH, this same correlation could not be identified for the late twentieth century (Wiedenmann et al. 2002), but could for the early twenty-first century (Lupo et al. 2019) and the entire data set overall. Many have demonstrated a connection between the dynamic character of the mid-latitude storm tracks and blocking (e.g., Lupo 2021 and references therein).

Wiedenmann et al. (2002) found that the global trends and variability in extratropical cyclones found by Key and Chan (1999) matched their overall trend and variability in the number of blocking events. Given the dynamic connection between these two phenomena, more extratropical cyclone activity would correspond to increased chances of block formation or duration. Tillinina et al. (2013) and Wang et al. (2016) studied cyclone counts in different reanalyses, and in spite of strong reanalysis differences in the counts, the NH and SH trends in cyclone occurrence or duration up to 2010 match the overall blocking trends here. This included the relative minimums for the 1980s and 1990s found in Lupo et al. (2019).

The decrease in rapidly deepening extratropical cyclones for the NH (e.g., Neu et al. 2013) is consistent with the decrease in NH BI found here. Tillinina et al. (2013) showed increases in the number of rapid deepening cyclones in the NH and North Atlantic until 1990, then a decrease from 1990 to 2010. They found the trends were enhanced in the north Pacific, except the turning point was closer to 2000. As stated in Sect. 3, BI decreased overall in the NH (Fig. 1) and does decrease especially among stronger blocks in the north Pacific and strong and weak Atlantic blocks (see Fig. 4). In the SH, Tillinina et al. (2013) find an increase in the number of rapid deepening cyclones up to 2010, which is consistent with the increase in stronger BI events overall (Fig. 7) and the southern Pacific (Fig. 10) where the majority of SH blocking occurs. The more persistent and more active block increases generally would also be consistent with more rapid deepening cyclones. This kind of detail would be more difficult to identify using the Lupo et al. (2019) methods.

Studies such as Wang et al. (2016) elucidate the difficulty in inferring extratropical cyclone trends due to the reanalysis data set used, and Neu et al. (2013) demonstrate that some results are dependent on the cyclone tracking methods used. Given the strong links between block occurrence, duration, and intensity and extratropical cyclone occurrence and deepening rate, it is proposed here that the examination of blocking may be useful in reinforcing the results found for regional changes in extratropical cyclone character since blocking is a large-scale phenomenon and easier to detect. This could be especially true where studies find mixed results. More study regarding this topic should be performed.

5 Summary and conclusion

This study examined the trend analysis of atmospheric blocking characteristics by using Şen's ITA method for both the NH and SH. The blocking data archived at the University of Missouri includes BO, BD, blocking size, onset longitude, BI, and preferred location. Block intensity, occurrence, and duration are used in this study for the period of 1968–2019 for the NH and 1970–2019 for the SH. The NCEP–NCAR reanalysis 500 hPa geopotential height data is used to detect blocking in this dataset. Şen's ITA method is a non-parametric trend test which is performed visually. The data under consideration is separated into two equal parts and then compared on Cartesian coordinates.

The BI has a decreasing trend for all clusters over the entire NH and the Atlantic Region. In the Pacific Region, the weak cluster has an increasing trend while the medium cluster is closer to the trend-free line. The Continental Region has a decreasing trend for all three clusters except the lower part of the low cluster, which has an increasing trend. Only the decreasing trend for the Continental Region BI is statistically significant at 95% level according to the Mann–Kendall trend test. BD has an increasing trend for the whole NH for all clusters. Almost all the BD clusters of three preferred blocking locations have an increasing trend. According to the Mann–Kendall test, all the trend values are statistically significant at 99% level. The BO shows an increasing trend generally for all clusters in the less active cluster for the whole NH and each region. All the trend values are statistically significant at the 99% level, according to the Mann–Kendall test. The results of the Mann–Kendall test here update the inferred trends found in Lupo et al. (2019).

For the entire SH, the BI has a different trend behavior for different clusters as shown in section three. For the Atlantic Region, BI has an increasing trend for the lower part of the medium cluster while it is decreasing for strong values. In the Pacific and Indian Regions, all BI clusters have an increasing trend with lower trend magnitudes, generally. The trend for SH BI is not statistically significant.

All three clusters have an increasing trend for BD for the entire and for each region in general. SH. The exception is in the Indian Ocean Region where the more persistent cluster has decreasing trend with lower values and an increasing trend for the highest values in the more persistent cluster. According to the Mann–Kendall test, trends in BD are statistically significant within the whole SH and Atlantic and Pacific regions at 90%, 95%, and 95% levels, respectively. The BO has an increasing trend for the whole SH and Pacific Region generally where most blocking occurs. The Atlantic Region has no trend for small values within the medium cluster and an increasing trend for higher values with low magnitudes. The more active cluster has a decreasing trend for small values and an increasing trend for high values with low trend magnitudes. The Indian Region has a decreasing trend for small values within the medium cluster and an increasing trend for higher values within the cluster. The more active cluster has an increasing trend for lower values and the trend magnitude decreases in this region.

Finally, it is suggested here that the Şen's ITA is a simple methodology that can provide more detail regarding the trends and statistical associations in blocking character found by earlier studies. The ITA methodology demonstrates that the statistical character of weaker or less persistent blocking events can be different from those of stronger events. It is also proposed that using the ITA analysis to examine trends in the character of blocking can reinforce regional changes found by those examining extratropical cyclone characteristics and vice-versa.

Author contribution Conceptualization: BE, ARL; literature search: BE, ARL; data analysis: BE, ARL; writing — original draft preparation: BE, ARL.

Data Availability The research data will be available upon request.

Code availability Not applicable.

Declarations

Ethics approval Not applicable.

Consent to participate Not applicable.

Consent for publication Not applicable.

Competing interests The authors declare no competing interests.

References

Aalijahan M, Salahi B, Rahimi YG, Asl MF (2018) A new approach in temporal-spatial reconstruction and synoptic analysis of cold waves in the northwest of Iran. Theor Appl Climatol. https://doi.org/10.1007/s00704-018-2601-7

Barnes EA, Dunn-Sigouin E, Masato G, Woollings TJ (2014) Exploring recent trends in Northern Hemisphere blocking. Geophys Res Lett 41:638–644. https://doi.org/10.1002/2013GL058745

Barriopedro D, García-Herrera R, Lupo AR, Hernández E (2006) A climatology of northern hemisphere blocking. J Clim 19(6):1042–1063. https://doi.org/10.1175/JCLI3678.1

Brunner L, Schaller N, Anstey J, Sillmann J, Steiner AK (2018) Dependence of present and future European temperature extremes on the location of atmospheric blocking. Geophys Res Lett 45:6311–6320. https://doi.org/10.1029/2018GL077837

Canyılmaz MG, Efe B (2020) Atmospheric blocking and heat-cold waves relationship in Edirne, Tekirdağ, Kırklareli and Istanbul provinces. J Anatol Environ Animal Sci 5(4):611–617. https://doi.org/10.35229/jaes.798781

Cui L, Wang L, Lai Z, Tian Q, Liu W, Li J (2017) Innovative trend analysis of annual and easonal air temperature and rainfall in the Yangtze River Basin, China during 1960–2015. J Atmos Sol Terr Phys 164:48–59

Efe B, Lupo AR, Deniz A (2019) The relationship between atmospheric blocking and precipitation changes in Turkey between 1977 and 2016. Theor Appl Climatol 138:1573–1590. https://doi.org/10.1007/s00704-019-02902-z

Efe B, Sezen I, Lupo AR, Deniz A (2020) The relationship between atmospheric blocking and temperature anomalies in Turkey between 1977 and 2016. Int J Climatol 40(2):1022–1037. https://doi.org/10.1002/joc.6253

Efe B, Lupo AR, Deniz A (2020) Extreme temperatures linked to the atmospheric blocking events in Turkey between 1977 and 2016. Nat Hazards 104(2):1879–1898. https://doi.org/10.1007/s11069-020-04252-w

Kendall MG (1975) Rank correlation methods. Oxford University Press, New York, NY

Khodayar S, Kalthoff N, Kottmeier C (2018) Atmospheric conditions associated with heavy precipitation events in comparison to seasonal means in the western Mediterranean region. Clim Dyn 51:951–967. https://doi.org/10.1007/s00382-016-3058-y

Key JR, Chan ACK (1999) Multidecadal global and regional trends in 1000 mb and 500 mb cyclone frequencies. Geophys Res Lett 26:2053–2056

Lejenas H, Okland H (1983) Characteristics of Northern Hemisphere blocking as determined from a long time series of observational data. Tellus A 35(5):350–362. https://doi.org/10.3402/tellusa.v35i5.11446

Lhotka O, Kyselý J, Plavcová E (2018) Evaluation of major heat waves' mechanisms in EURO-CORDEX RCMs over Central Europe. Clim Dyn 50:4249–4262. https://doi.org/10.1007/s00382-017-3873-9

Lupo AR (2021) Atmospheric blocking events: a review Annals of the New York Academy of Sciences, Special Issue: the Year in Climate. Sci Res 2021:5–24

Lupo AR, Smith PJ (1995) Climatological features of blocking anticyclones in the Northern Hemisphere. Tellus A 47(4):439–456. https://doi.org/10.1034/j.1600-0870.1995.t01-3-00004.x

Lupo AR, Jensen AD, Mokhov II, Timazhev AV, Eichler T, Efe B (2019) Changes in global blocking character during the most recent decades. Atmos 10(19):00092

Matsueda M (2011) Predictability of Euro-Russian blocking in summer of 2010. Geophys Res Lett 38:L06801. https://doi.org/10.1029/2010GL046557

Mokhov II, Akperov MG, Prokofyeva MA, Timazhev AV, Lupo AR, Le Treut H (2012) Blockings in the Northern Hemisphere and Euro-Atlantic region: estimates of changes from reanalyses data and model simulations. Doklady 449:430–433

Moravej M, Karimirad I, and Ebrahimi K (2018) Spatio-temporal analysis of the Karun River water quality. Inter J Water 12(3). https://doi.org/10.1504/IJW.2018.093669

Neu U et al (2013) IMILAST: a community effort to intercompare extratropical cyclone detection and tracking algorithms. Bull Amer Meteor Soc 94:529–547. https://doi.org/10.1175/bams-d-11-00154.1

Oliveira FNM, Carvalhoc LMV, Ambrizzi T (2014) A new climatology for southern hemisphere blockings in the winter and the combined effect of ENSO and SAM phases. Int J Climatol 34:1676–1692

O'Reilly CH, Minobe S, Kuwano-Yoshida A (2016) The influence of the Gulf Stream on wintertime European blocking. A Clim Dyn 47:1545. https://doi.org/10.1007/s00382-015-2919-0

Phuong DND, Hai LM, Dung HM et al (2022) Temporal trend possibilities of annual rainfall and standardized precipitation index in the Central Highlands, Vietnam. Earth Syst Environ 6:69–85. https://doi.org/10.1007/s41748-021-00211-y

Pinheiro MC, Ullrich PA, Grotjahn R (2019) Atmospheric blocking and intercomparison of objective detection methods: flow field characteristics. Clim Dyn 53:4189–4216

R Core Team (2018) R: A language and environment for statistical computing. R Foundation for Statistical Computing, Vienna, Austria. Retrieved https://www.R-project.org/. Accessed 1 Feb 2021

Rabinowitz JL, Lupo AR, Guinan PE (2018) Evaluating linkages between atmospheric blocking patterns and heavy rainfall events across the north-central Mississippi River valley for different ENSO phases. Adv Meteorol 2018:1217830. https://doi.org/10.1155/2018/1217830

Renwick JA, Revell MJ (1999) Blocking over the South Pacific and Rossby wave propagation. Mon Weather Rev 127(10):2233–2247. https://doi.org/10.1175/1520-0493(1999)127<2233:BOTSPA>2.0.CO;2

Şen Z (2012) Innovative trend analysis methodology. J Hydrol Eng 17(9):1042–1046. https://doi.org/10.1061/(ASCE)HE.1943-5584.0000556

Şen K, Aksu H (2021) Trend analysis of observed standard duration maximum precipitation for Istanbul. Teknik Dergi 32(1):10495–10514. https://doi.org/10.18400/tekderg.647558(inTurkish)

Sitnov SA, Mokhov II, Lupo AR (2014) Evolution of the water vapor plume over Eastern Europe during summer 2010 atmospheric blocking. Adv Meteorol 2014:1–11. https://doi.org/10.1155/2014/253953

Tibaldi S, Molteni F (1990) On the operational predictability of blocking. Tellus A 42(3):343–365

Tilinina N, Gulev SK, Rudeva I, Koltermann P (2013) Comparing cyclone life cycle characteristics and their interannual variability in different reanalyses. J Clim 26:6419–6438. https://doi.org/10.1175/jcli-d-12-00777.1

Tosunoglu F, Kisi O (2017) Trend analysis of maximum hydrologic drought variables using Mann-Kendall and Şen's innovative trend method. River Res Appl 33(4):597–610

University of Missouri Blocking Archive. Available online: http://weather.missouri.edu/gcc. Accessed 30 Dec 2020

Wang XL, Feng Y, Chan R, Isaac V (2016) Inter-comparison of extratropical cyclone activity in nine reanalysis datasets. Atmos Res 181:133–153. https://doi.org/10.1016/j.atmosres.2016.06.010

Wickham H (2016) ggplot2: elegant graphics for data analysis. Springer-Verlag, New York. Retrieved http://ggplot2.org. Accessed 1 Feb 2021

Wickham H, Francios R, Henry L, Müller K (2018) Dplyr: a grammar of data manipulation. Retrieved https://cran.r-project.org/package=dplyr. Accessed 1 Feb 2021

Wiedenmann JM, Lupo AR, Mokhov II, Tikhonova EA (2002) The climatology of blocking anticyclones for the Northern and Southern Hemisphere: block intensity as a diagnostic. J Clim 15:3459–3474

Terms and Conditions

Springer Nature journal content, brought to you courtesy of Springer Nature Customer Service Center GmbH (“Springer Nature”).
Springer Nature supports a reasonable amount of sharing of research papers by authors, subscribers and authorised users (“Users”), for small-scale personal, non-commercial use provided that all copyright, trade and service marks and other proprietary notices are maintained. By accessing, sharing, receiving or otherwise using the Springer Nature journal content you agree to these terms of use (“Terms”). For these purposes, Springer Nature considers academic use (by researchers and students) to be non-commercial.
These Terms are supplementary and will apply in addition to any applicable website terms and conditions, a relevant site licence or a personal subscription. These Terms will prevail over any conflict or ambiguity with regards to the relevant terms, a site licence or a personal subscription (to the extent of the conflict or ambiguity only). For Creative Commons-licensed articles, the terms of the Creative Commons license used will apply.
We collect and use personal data to provide access to the Springer Nature journal content. We may also use these personal data internally within ResearchGate and Springer Nature and as agreed share it, in an anonymised way, for purposes of tracking, analysis and reporting. We will not otherwise disclose your personal data outside the ResearchGate or the Springer Nature group of companies unless we have your permission as detailed in the Privacy Policy.
While Users may use the Springer Nature journal content for small scale, personal non-commercial use, it is important to note that Users may not:

1. use such content for the purpose of providing other users with access on a regular or large scale basis or as a means to circumvent access control;
2. use such content where to do so would be considered a criminal or statutory offence in any jurisdiction, or gives rise to civil liability, or is otherwise unlawful;
3. falsely or misleadingly imply or suggest endorsement, approval , sponsorship, or association unless explicitly agreed to by Springer Nature in writing;
4. use bots or other automated methods to access the content or redirect messages
5. override any security feature or exclusionary protocol; or
6. share the content in order to create substitute for Springer Nature products or services or a systematic database of Springer Nature journal content.

In line with the restriction against commercial use, Springer Nature does not permit the creation of a product or service that creates revenue, royalties, rent or income from our content or its inclusion as part of a paid for service or for other commercial gain. Springer Nature journal content cannot be used for inter-library loans and librarians may not upload Springer Nature journal content on a large scale into their, or any other, institutional repository.
These terms of use are reviewed regularly and may be amended at any time. Springer Nature is not obligated to publish any information or content on this website and may remove it or features or functionality at our sole discretion, at any time with or without notice. Springer Nature may revoke this licence to you at any time and remove access to any copies of the Springer Nature journal content which have been saved.
To the fullest extent permitted by law, Springer Nature makes no warranties, representations or guarantees to Users, either express or implied with respect to the Springer nature journal content and all parties disclaim and waive any implied warranties or warranties imposed by law, including merchantability or fitness for any particular purpose.
Please note that these rights do not automatically extend to content, data or other material published by Springer Nature that may be licensed from third parties.
If you would like to use or distribute our Springer Nature journal content to a wider audience or on a regular basis or in any other manner not expressly permitted by these Terms, please contact Springer Nature at

onlineservice@springernature.com